



“Josef Stefan”
Institute

Liquid crystal in confined environment

Adviser: Prof. Rudi Podgornik

Supervisor: Prof. Igor Muševič

By

Maryam Nikkhou

September 2011

Contents

Abstract	1
1. Introduction	2
2. Free energy	2
3. Confinement	4
3.1 Liquid crystal in curved geometry	4
3.2 Liquid crystal between two flat plates	6
4. Effect of alignment on nematic liquid crystal	8
4.1 Semi-infinite sample problem	8
4.2 Finite thickness sample problem	13
5. Conclusion	15
6. References	16

Abstract

Free energy of liquid crystal and different confinement geometries such boundary conditions enforced by planar substrates or curved boundary conditions are investigated. The effect of confinement on the orientational order parameter of nematic liquid crystal is examined in the framework of Landau-de Gennes theory by assuming a large surface orientation potential. Calculations are presented for both the semi-infinite-sample case and the finite-thickness-sample case. Variation phase diagrams are discussed to show the effect of sample thickness and substrate potential on the bulk as well as boundary-layer phase-transition temperature.

1. Introduction

Studies of the influence of confinement and random substrate disorder on physical properties are topic of current interest. Such studies are particularly important for liquid crystal system since their weak orientational and translational order is considerably influenced by the presence of surface. In addition, because of the existence of long-range correlations near a phase transition, liquid crystals are a unique and rich system to test in restricted geometries [1]. On the technological side, the advances have also been spectacular: liquid crystal displays, thermometers, optical imaging and other application. For many of these utilities we have to confine liquid crystal to use them. These means we put sample between borders of some kind and some exact geometry. To understand how different technology work and to invent new applications it is important to understand theory that describes confined liquid crystals [2].

There are several theoretical and few experimental studies on the confinement effect on the orientational order parameter, phase transition, and specific heat of nematic liquid crystal enclosed inside the walls of different geometries [1, 3-7].

2. Free energy

In a given microscopic region of a liquid crystal there is a definite preferred molecular axis. Even in equilibrium the direction of this axis can vary from place to place, and it can be forced to vary by the action of external forces or boundary conditions. This variation is described by vector function $n(r)$, where $|n| = 1$. We will refer to the deformation of relative orientations away from the equilibrium position as curvature strains. Restoring forces which arise to oppose deformations are then called curvature stresses or torques.

Let us consider a uniaxial liquid crystal. We assume that n varies slowly from point to point, and thus is defined by continuity at other points in the region. At r we introduce local right-handed Cartesian coordinate system x, y, z with n parallel to z . We define curvature strains.

$$\text{Splay: } \frac{\partial n_x}{\partial x} = a_1, \quad \frac{\partial n_y}{\partial y} = a_2 \quad (1)$$

$$\text{Twist: } -\frac{\partial n_y}{\partial x} = a_3, \quad \frac{\partial n_x}{\partial y} = a_4 \quad (2)$$

$$\text{Bent: } \frac{\partial n_x}{\partial z} = a_5, \quad \frac{\partial n_y}{\partial z} = a_6 \quad (3)$$

these quantities measure director deformation. The curvature strains represent three different distortion types of the director. Called splay, twist, bend, see Fig. 1.

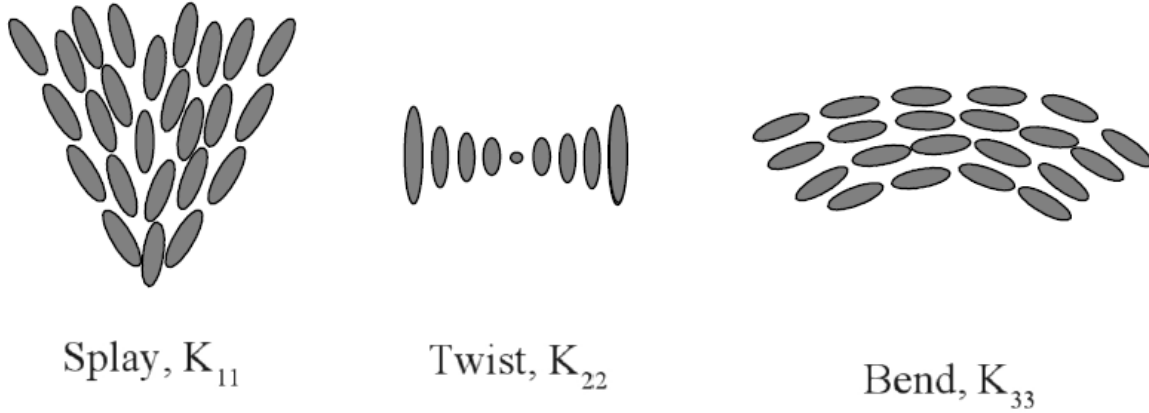


Figure 1. The three principal types of deformation in nematic liquid crystal.

We postulate that the Gibbs free energy density of a liquid crystal, relative to its free energy density in the state of uniform orientation, can be expanded in terms of the six curvature strains:

$$f = \sum_{i=1}^6 k_i a_i + \frac{1}{2} \sum_{i,j=1}^6 k_{ij} a_i a_j \quad (4)$$

Fortunately, there are restrictions on the free energy that reduce the number of independent constants k_i , k_{ij} . First there can be no term for which n and $-n$ give different energy values. Second, there can be no linear terms. These terms change if the coordinate system is rotated about the director, if the director is reversed, or if the coordinate system is inverted. Finally, terms that can be written as divergence and integrated over the volume of the sample can be changed to a surface integral. These contributions to the free energy must be taken into account when considering surface effects, but in most cases can be ignored in a discussion of the volume free energy per unit volume.

The free energy per unit volume of nematic liquid crystal can be written as follows,

$$f = \frac{1}{2} k_{11} (\nabla \cdot n)^2 + \frac{1}{2} k_{22} (n \cdot (\nabla \times n))^2 + \frac{1}{2} k_{33} (n \times (\nabla \times n))^2 \quad (5)$$

k_{11} , k_{22} and k_{33} are called elastic constants (or Frank constants). These three constants describe how 'stiff' the liquid crystal is to distortion of the director for each of the characteristic deformation modes shown in Fig. 1. They are temperature dependent, $k_{ii} \propto S^2(T)$, where S is order parameter. Typical values of these constants are about 10^{-11} J/m , with K_{33} being two or three times larger than K_{11} and K_{22} .

The equilibrium state of the liquid crystal is obtained by minimizing the total free energy

$$F = \int_V f \left(n_i, \frac{\partial n_i}{\partial x_j} \right) d\mathbf{r} \quad (6)$$

With appropriate boundary conditions and subject to the condition $n^2 = 1$. Allowing n_i to vary in Eq.6, we know Euler-Lagrange equations

$$-\frac{\partial}{\partial x_i} \frac{\partial f}{\partial \frac{\partial n_i}{\partial x_i}} + \frac{\partial f}{\partial n_i} = \gamma n_i \quad (7)$$

where γ is Lagrange multiplier due to constrain $n^2 = 1$ [2].

3. Confinement

The confinement of liquid crystals imposed by surface boundary conditions is at the heart of most liquid crystal device applications. This confinement can come in the form of boundary conditions enforced by planar substrates or curved boundary conditions.

3.1 Liquid crystal in curved geometry

Interest in liquid crystalline materials confined to curved geometries has expanded greatly in recent years because of their important role in new and emerging electro-optic technologies and their richness in physical phenomena. The discovery of the usefulness of these materials, conspicuous in electrically controllable light scattering windows and reflective mode display technology, has burgeoned into a mature reflective display technology and heralded an era of fascination with the confinement organized fluids. Independent of the method used to constrain liquid crystals, phase separation, encapsulation, or permeation; these systems have one underlying common theme: a symmetry-breaking, non-planar confinement imposed by the surrounding matrix. In addition, confined liquid crystal systems differ from macroscopic bulk liquid crystals because of their large surface-to-volume ratio [1]. When sample is closed inside sphere made of some suitable substance (polymer). Liquid crystal again order inside the droplet according to boundary condition. In spherical confinement the configuration strongly depends on the delicate interplay between surface and elastic forces. For the homeotropic aligned droplets (Fig. 2), several configurations are possible:

- (1) The radial (splay-elastic deformation, k_{11});
- (2) The axial with defects (splay-bend configuration, $k_{11} - k_{33}$);

For the homogeneous aligned droplets in Fig. 2, there are several other configuration:

- (1) The bipolar configuration with defects at the poles (splay-bend configuration, $k_{11} - k_{33}$);

(2) The aligned bipolar configuration when an electric field is applied to a material with a positive dielectric anisotropy ($\Delta\varepsilon > 0$, splay-bend configuration $k_{11} - k_{33}$);

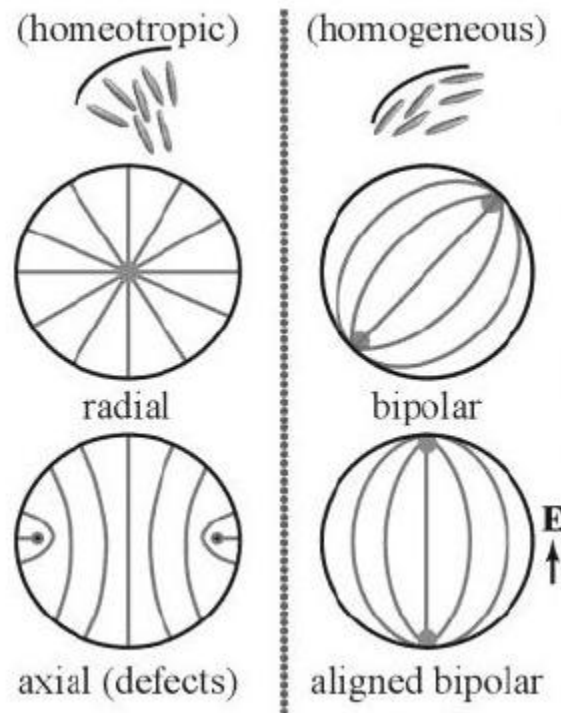


Figure 2: Examples of liquid crystals confined to spherical droplets.

Liquid crystal can also be confined to cylinders, as shown in Fig. 3. When homeotropic alignment persists, radial (splay, k_{11}), planar polar (splay-bend, $k_{11} - k_{33}$) configurations are possible [8].

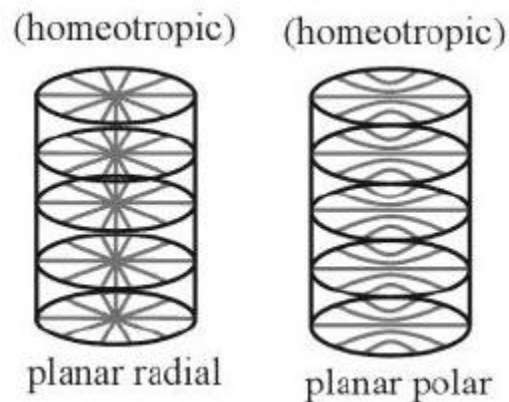


Figure 3: Examples of liquid crystals confined to cylinders.

3.2 Liquid crystal between two flat plates

Our discussion is more about liquid crystal between two flat plates, the simplest one but not least useful. Such studies on nematic liquid crystals are important both from fundamental and technological points of view. For example, nematic liquid crystal is sandwiched between two parallel glass plates for display (LCD) applications.

To see how theory from sect. 2 works let us consider an example. Being with the most simple geometry possible, Fig. 4. Imagine that liquid crystal is sandwiched between two flat glass plates separated by a distance d . The z axis is perpendicular to glass surface. Let us call the angle between the director and x -axis $\theta(z)$; then $n = (\cos \theta, \sin \theta, 0)$. In general, the energy associated with distortion involves splay, twist and bend. Calculated terms are

$$\nabla \cdot n = 0, \quad n \cdot (\nabla \times n) = -\cos^2 \theta \frac{d\theta}{dz} - \sin^2 \theta \frac{d\theta}{dz}, \quad n \times (\nabla \times n) = 0 \quad (8)$$

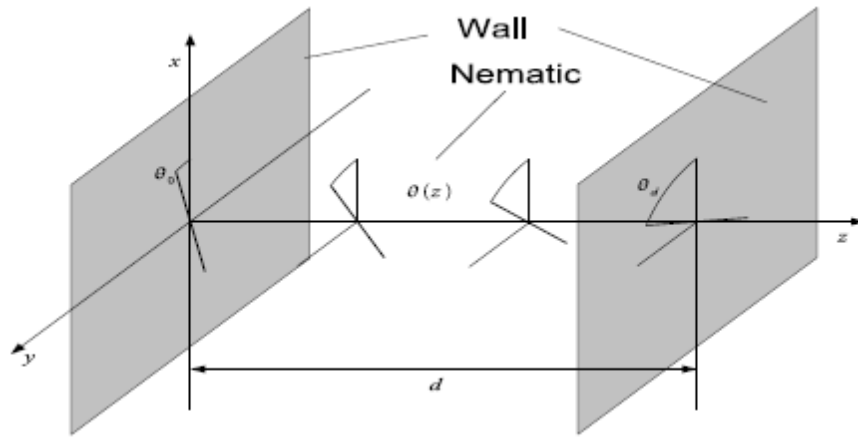


Figure 4: twist nematic cell. On the left wall there is easy axis along direction θ_0 , on the right wall easy axis is along θ_d .

Using these results in Eq. 4 one has

$$f = \frac{1}{2} k_{22} \left(\frac{d\theta}{dz} \right)^2 \quad (9)$$

Now we follow the procedure presented at the end of Sec. 2, and the appropriate Euler equation is

$$\frac{d}{dz} \frac{\partial f}{\partial \frac{d\theta}{dz}} - \frac{\partial f}{\partial \theta} = 0$$

Substituting the expression for f into this equation yields

$$k_{22} \frac{d^2\theta}{dz^2} = 0, \quad \text{and,} \quad \theta = Az + B \quad (10)$$

We see that θ is linear function of z with y -interception $B = \theta(0)$ and slope $d\theta/dz = A = [\theta(d) - \theta(0)]/d$. This solution is good only for strong anchoring and in the bulk area. This means that θ is fixed at $z = 0$ and $z = d$ because the surface forces are strong enough to impose a well-define direction to the director n . In real situation it can happen that this is not true one deals with weak anchoring on one or on both walls. In this case Eq. 9 no longer holds. Weak anchoring can be modeled by an appropriate phenomenological surface term, which increases energy if director is not aligned with easy axis, e.g.

$$f_{surf} = \frac{W}{2} \sin^2(\theta(0) - \theta_0) \quad (11)$$

where W is surface term strength and θ_0 is easy axis. Suppose that we have weak anchoring only at $z = 0$, in this case we have

$$F_s = F_A + F_{surf} = \int_0^d \frac{1}{2} k_{22} \left(\frac{d\theta}{dz} \right)^2 dz + \frac{W}{2} \sin^2(\theta(0) - \theta_0) \quad (12)$$

For that kind of energy a possible solution for $\theta(z)$ is shown on Fig. 5. To estimating the anchoring strength we define, Fig. 5, extrapolation length b . We will not derive $\theta(z)$ and b at surface from microscopic calculations but we can obtain estimate of b by estimating Eq.5 hold down to the surface and at surface we add appropriate term

$$f_s = \frac{1}{2} k_{22} d \left(\frac{\theta(d) - \theta(0)}{d} \right)^2 + \frac{W}{2} \theta^2(0), \quad \sin(\theta) \approx \theta \text{ because } \theta \ll 1 \quad (13)$$

Minimizing this with respect to $\theta(0)$ we find

$$\theta(0) = \frac{k_{22}}{W} \frac{\partial \theta}{\partial z}$$

Comparing equation with the definition of b we see that, in our approximation

$$b = \frac{k_{22}}{W}$$

This length is a good measure of how strong anchoring is in comparison with elastic constant k_{22} . This is the fundamental formula for boundary effects. We have two possibility: strong anchoring, if b is comparable to the molecular a , this means that ratio $F_A/F_{surf} = b/d \sim a/d$. For weak anchoring, extrapolation length may become much larger than the molecular dimensions a and angle $\theta(0)$ is large [2].

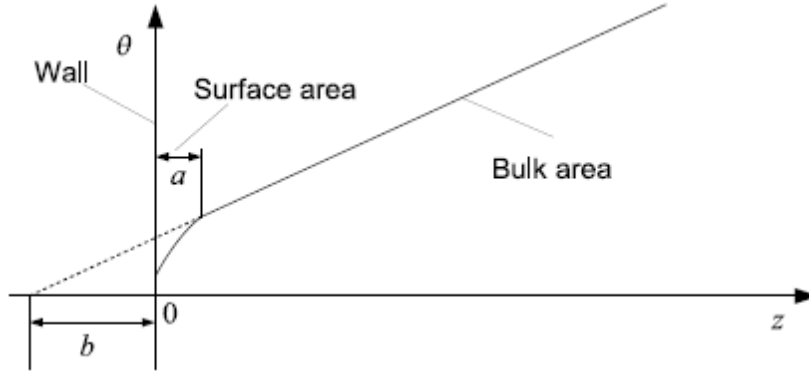


Figure 5: depiction of $\theta(z)$ minimizing free energy Eq. 12. In region of molecular thickness a near the surface area the twist depends on detailed molecular properties. b is the extrapolation length.

4. Effect of alignment on nematic liquid crystal

Now we consider the effect of confinement on the order parameter of nematic liquid crystals due to the alignment at the walls. Ping Sheng has calculated the order parameter profile in thin cells using the Landau de Gennes theory assuming a surface potential, which enhances the order parameter at surface.

4.1 Semi-infinite sample problem

Consider a sample of nematic liquid crystal bounded on one side by a substrate. The solid-liquid crystal interface is defines as $z = 0$, and the sample is assumed to be uniform in x and y directions. The substrate is treated so that the nematic liquid crystal molecules in its immediate vicinity experience an uniaxial aligning potential along some fixed spatial direction \hat{n} . The potential felt by each molecule can expressed in general as

$$v(\theta, z) = G\delta(z)[P_2(\cos \theta) + bP_4(\cos \theta) + cP_6(\cos \theta)] \quad (14)$$

where θ is the angle between the long axis of the molecule, \hat{n} , z is the normal distance from the substrate, G is a constant denoting the strength of the potential, P_{2n} denotes even-order Legendre polynomials, and b, c , etc., are the series expansion coefficients for the angular part of the series expansion coefficients for the angular part of the potential. In Eq. 13, it is assumed that the surface potential is short range as indicated by the delta function. If, in addition, $v(\theta, z)$ is truncated to the leading term of the series and averaged over the many molecules within a small spatial region, then the resulting form of the macroscopic potential is given by

$$V = \langle v(\theta, z) \rangle = -G\delta(z)\langle P_2(\cos \theta) \rangle = -G\delta(z)S \quad (15)$$

To study the thermodynamic consequences of such a substrate potential, we start with the Landau-de Gennes free-energy density ϕ :

$$\phi = f(S) + L \left(\frac{ds}{dz} \right)^2 - \frac{G}{A} \delta(z)S \quad (16)$$

$$f(S) = a(T - T^*)S^2 + BS^3 + CS^4 \quad (17)$$

where T is the temperature, a, T^*, B, C and L are material parameters which can be determined from thermodynamic and fluctuation measurements, and A is the area of the planar substrate. Given ϕ , the total free energy Φ is obtained directly by integration over z :

$$\frac{\Phi}{A} = \int_0^\infty \left[f(S) + L \left[\frac{dS}{dz} \right]^2 \right] dz - \frac{G}{A} S_0 \quad (18)$$

where S_0 denotes the value of S at $z = 0$. To determine the equilibrium form of $S(z)$, we employ the condition of minimum free energy. The minimization procedure involves two steps: First, S_0 is held fixed and the integral in Eq. 18 is minimized variationally with respect to $S(z)$. The resulting expression for Φ is then minimized with respect to S_0 . Implementation of the first step results in the Euler equation

$$f'(S) = 2L \left(\frac{d^2S}{dz^2} \right)$$

which can be integrated once to yield

$$L \left(\frac{dS}{dz} \right)^2 = f(S) + K \quad (19)$$

The constant K is determined by the condition that at $z \rightarrow \infty$, the bulk liquid crystal is uniform and, therefore,

$$\left. \frac{dS}{dz} \right|_{z \rightarrow \infty} = 0 \quad (20)$$

which directly implies

$$\xi_0^2 \left(\frac{dS}{dz} \right)^2 = F(S) - F(S_b) \quad (21)$$

Here $\xi_0 \equiv (L/aT_K^0)^{1/2}$ is the correlation length, $F(S) \equiv f(S)/aT_K^0$, and S_0 is the bulk value of the order parameter. Substitution of Eq. 21 into Eq. 18 yields

$$\frac{\Phi}{AaT_K^0} = F(S_b)D + \xi_0 \left[2 \int_{S_0}^{S_0} \sqrt{F(S) - F(S_b)} dS - gS_0 \right] \quad (22)$$

The equilibrium value of S_0 is determined by the condition $d\Phi_{BL}/dS_0 = 0$, or

$$F(S_0) = F(S_b) + \frac{g^2}{4} \quad (23a)$$

where S_b is found by the stipulation that

$$F(S_b) = \min F(S) \quad (23b)$$

where min represents the absolute minimum of $F(S)$. In case Eq. 23 has multiple roots, the correct S_0 is that one which gives the lowest value of Φ_{BL} as expressed by Eq. 22. Once S_0 is found, the $S(z)$ profile can be obtained through the integral of Eq. 20, or

$$\frac{z}{\xi_0} = \int_{S(z)}^{S_0} \frac{dS}{\sqrt{F(S) - F(S_b)}} \quad (24)$$

The calculated results of S_0 as a function of temperature for the nematic liquid crystal 4-penty-4'-cyanobiphenyl (PCB) is shown in Fig. 6. In the calculation, measured values $a = 0.065 \text{ J/cm}^3\text{K}$, $B = -0.53 \text{ J/cm}^3$, $C = 0.98 \text{ J/cm}^3$, $T^* = 307.14 \text{ K}$, and $L = 4.5 \times 10^{-14} \text{ J/cm}$ were used []. It is seen that for $g < 0.0056$, S_0 experiences a discontinuous

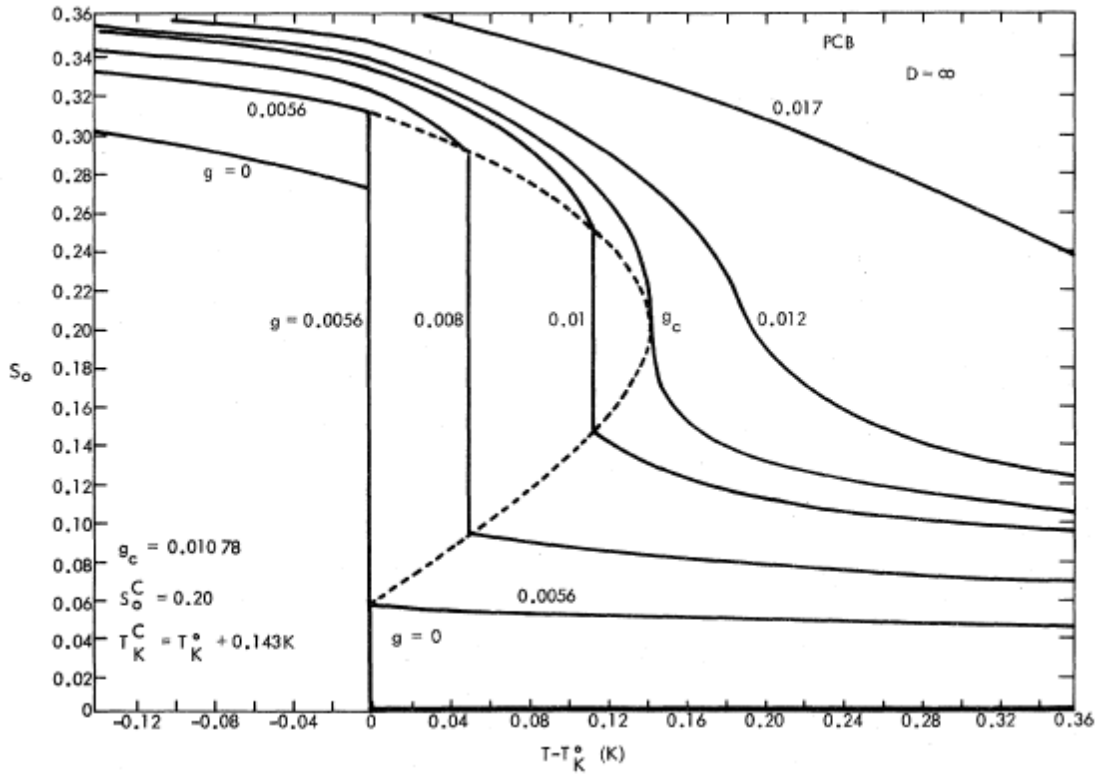


Figure 6. Calculated PCB order-parameter value at the substrate-nematic interface as a function of temperature. Magnitude of the substrate potential is labeled beside each curve. Values of the critical point parameters are noted in the figure.

transition in its value at bulk-transition temperature T_K^0 . However, at $0.0056 = g_0 < g < g_c = 0.012$, the transition of S_0 occurs at a temperature higher than T_K^0 . At $g > g_c$, the transition disappears and the variation of S_0 becomes a continuous function of temperature. The nature of the transition at $g > g_c$ and in the range $g_0 < g < g_c$ deserves closer scrutiny. The behavior of the boundary layer for $g = 0.004$ is shown in Fig. 7. At $T = T_K^0$, it is seen that both S_0 and S_b experience a discontinuous jump as indicated by the two curves corresponding to $S(z)$ just before and just after the transition. The simultaneous transition of S_0 and S_b is understandable since the value of S_0 is linked to the bulk S_b by elastic forces [represented by the $L(dS/dz)^2$ term in the free-energy density] and in the limit of weak substrate potential the transition in S_0 is induced by the bulk transition. At $g = 0.008 > g_0$, however, a different type of boundary-layer behavior is predicted as illustrated in Fig. 8. Fig. 8(a) shows the $S(z)$ just before and just after the bulk transition at T_K^0 . Although S_b has a discontinuous jump, S_0 stays fixed. At $T = T_K^0 + 0.049$, on the other hand, the value of S_0 exhibits a discontinuous transition while S_b stays unchanged ($=0$) as illustrated in Fig. 8(b). Since, in this case, the first-order transition involves only the boundary layer, the phase change shown in Fig. 8(b) is called as a boundary-layer phase transition. The physics of this occurrence is actually fairly simple. The

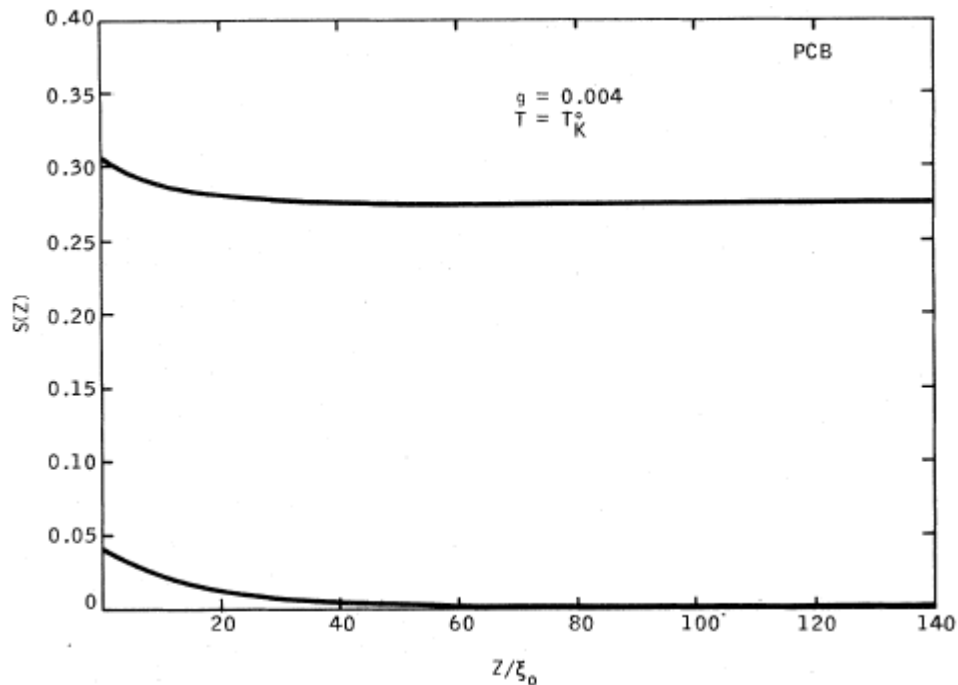


Figure 7. Variation of the order parameter S as a function of distance z/ξ_0 away from the substrate. Upper curve shows $S(z)$ just before the bulk transition at $T = T_K^0$, and lower shows $S(z)$ just after the transition. Value of the substrate potential $g = 0.004$ is noted in the figure.

layer of nematic molecules at the liquid crystal substrate interface experience two forces: the elastic force, which connects the surface molecules with the bulk, and the substrate aligning force. When the substrate potential is sufficiently strong, i.e., $g > g_0$ (but $g < g_c$), the increase in the elastic part of the free energy caused by the lowering of the bulk order-parameter value at T_K^0 cannot overcome the surface aligning potential. Therefore, S_0 stay unchanged. However, as temperature increases beyond T_K^0 , there is a point at which a trade off between the elastic free energy and the surface potential energy becomes advantageous and a boundary-layer transition occurs in which the gain in surface potential energy (resulting from the decrease of S_0) is offset by the lowering of the elastic free energy (and vice versa when T is lowered through the transition temperature) [3].

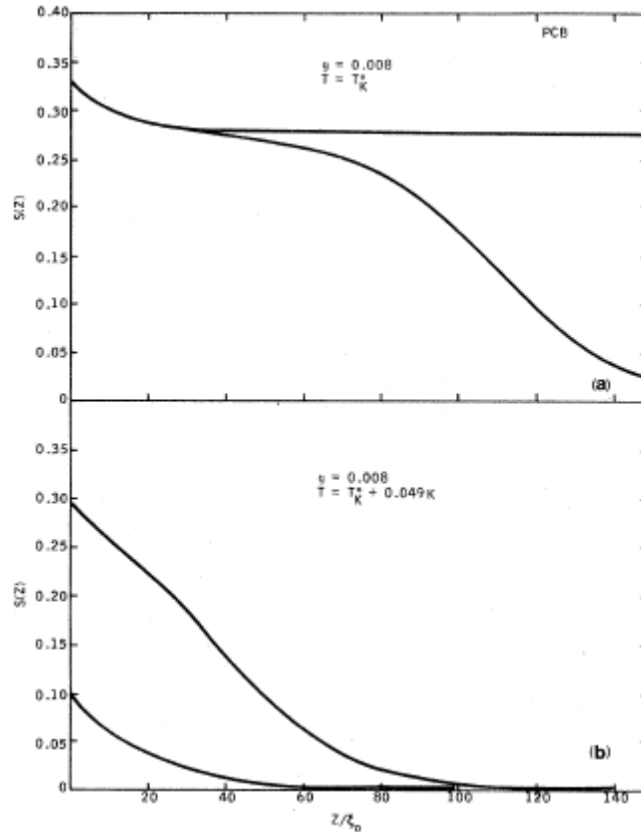


Figure 8. (a) Variation of the order parameters S as a function of distance z/ξ_0 away from the substrate. Two curves show $S(z)$ just before and just after the bulk transition at $T = T_K^0$. Magnitude of the substrate potential $g = 0.008$ is noted in the figure. In this case, the bulk order parameter has a discontinuous jump, but the value of S_0 stays fixed. (b) Variation of S as a function of z/ξ_0 at $T = T_K^0 + 0.049K$. Substrate potential is the same as in (a). Two curves correspond to $S(z)$ just before and just after a transition have occurred. Since in this case the transition involves only the boundary layer, it is labeled the boundary-layer phase transition.

4.2 Finite thickness sample problem

Consider a sample of nematic liquid crystal of uniform thickness $2D$ sandwiched between two identically treated substrates situation at $z = 0$ and $z = 2D$. Instead of the condition $dS/dz(z = \infty) = 0$ for the semi-infinite sample, in this case Sheng used $dS/dz(z = D) = 0$ due to the symmetry of the problem. Therefore, if the S_b denote the order parameter value at middle of the sample, i.e., $z = D$, then we are led to exactly Eq. 22, where Φ now stands for half of the total free energy of sample. However, due to the fact that D is finite, S_b and S_0 can no longer be decoupled as in the previous case. So he had to solve the coupled equations

$$F(S_0) - F(S_b) = \frac{g^2}{4} \quad (25a)$$

$$F'(S_b) \left(1 - \frac{\xi_0}{D} \int_{S_b}^{S_0} \frac{dS}{\sqrt{F(S) - F(S_0)}} \right) = 0 \quad (25b)$$

When there are multiple pairs of solutions (S_0, S_b) , the correct pair is always that one which gives the lowest value of Φ as expressed by Eq. 22. It should be noted that when $\xi_0/D \rightarrow 0$, Eq. 25 reduces to Eq. 23 for the semi-infinite case.

Through the use of the measured parameter values of PCB, Sheng has calculated the variations of S_b and S_0 as a function of T , g , and D . For $g = 0.008$, it is seen from Fig. 9 that transition temperature of S_b increases with decreasing D . As to S_0 , at $D/\xi_0 = 300$, it shows two transitions: the boundary-layer phase transition plus the one induced by the transition of S_b . We will label the transition which causes discontinuities in both S_0 and S_b as the ‘‘bulk transition,’’ in accordance with its limiting characterization as $D/\xi_0 \rightarrow \infty$. Since the boundary-layer transition temperature is found to be invariant with respect to D , the increasing bulk-transition temperature means that there is a thickness $D/\xi_0 = 160$, below which the boundary-layer transition disappears into the bulk transition. As D decreases even further, the first-order transition in both S_0 and S_b eventually turn into second-order transition at $D/\xi_0 = 15$. Results of similar calculations with $g = 0.012 > g_c$ are plotted in Fig. 10. In contrast to the semi-infinite case in which S_0 has no abrupt transition at this value of the substrate potential, for finite sample thickness S_0 always experiences a discontinuous jump coincident with the first-order transition in S_b . This behavior is similar to that for $g = 0.008$ at $D/\xi_0 < 160$. The critical thickness in this case occurs at $D/\xi_0 \approx 25$ [3].

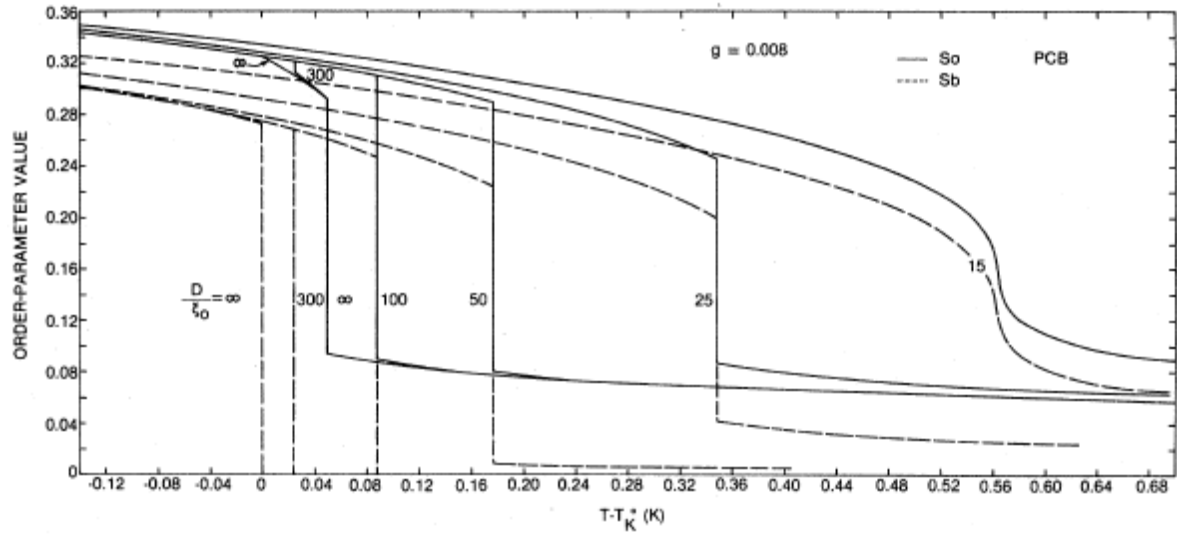


Figure 9. Variation of S_b (dashed curve) and S_0 (solid curve) as a function of temperature. The (half) thickness of the sample is labeled beside each curve. Magnitude of the substrate potential, $g = 0.008$, is noted in the figure.

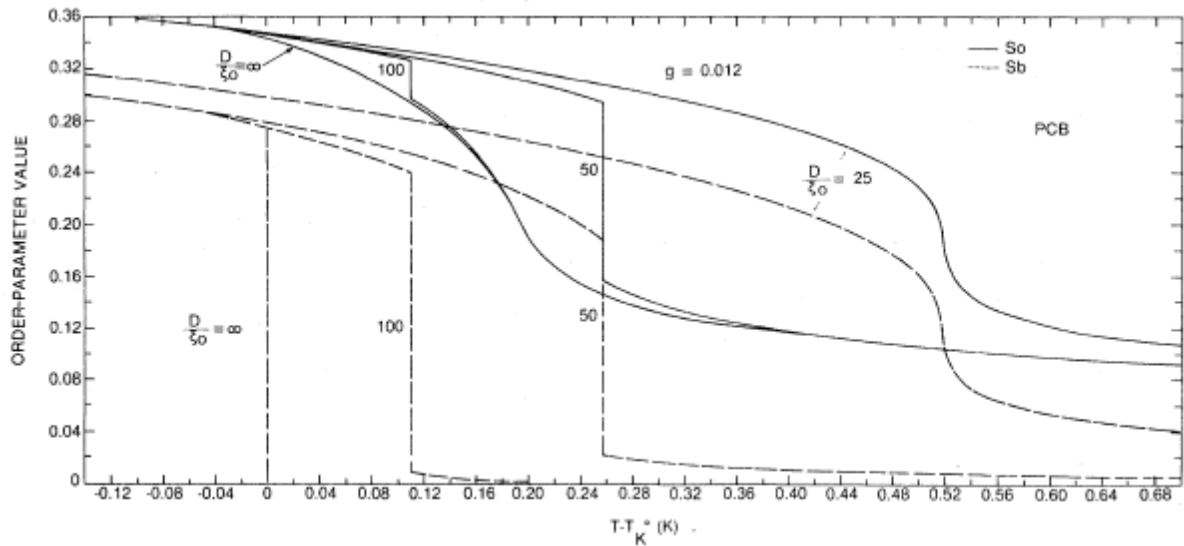


Figure 10. Variation of S_b (dashed curve) and S_0 (solid curve) as a function of temperature. The (half) thickness of the sample is labeled beside each curve. Magnitude of the substrate potential, $g = 0.012$, is noted in the figure.

5. Conclusion

In this seminar we discussed behavior of liquid crystals enclosed inside the walls of different geometries. The effect of confinement on the orientational order parameter of nematic liquid crystal in the framework of Landau-de Gennes theory assuming surface potential, which enhance the order parameter at surface has investigated. It is shown that the substrate potential, which can arise from surface treatment of liquid crystal display cells, not only induces a boundary layer in which the order-parameter values can be significantly different from that of the bulk, but also introduces a new boundary-layer phase transition which occurs at temperatures higher than the bulk-transition temperature. Various phase diagrams have presented to show the effects of sample thickness and substrate potential on the bulk as well as the boundary-layer phase-transition temperature.

6. References

- [1] G.P. Crawford, S. žumer, "Liquid crystals in complex geometry: Formed by polymer and porous networks", Taylor & Francis, (1996)
- [2] Luka Jeromel, "Confined liquid crystal", seminar, Ljubljana University, Ljubljana, (2011)
- [3] P. Sheng, "Boundary-layer phase transition in nematic liquid crystals", Phys. Rev. A, 26, 1610 (1982)
- [4] P. Sheng, "Phase transition in surface aligned nematic", Phys. Rev. Lett. 37, 1059 (1976).
- [5] K. Miyano, "Wall-induced pretransitional birefringence: a new tool to study boundary aligning forces in liquid crystals", Phys. Rev. Lett. 43, 51 (1979)
- [6] H. Mada, S. Kobayashi, "Surface and bulk order parameter of a nematic liquid crystal", Appl. Phys. Lett. 35(1), 4 (1979)
- [7] Z. Kutnjak, S. Kralj, g. Lahajnar , S. žumer, "Calorimetric study of octylcyanobiphenyl liquid crystal confined to controlled-pore glass", Phys. Rev. E, 68, 021705 (2003)
- [8] S. J. Woltman, G. D. Jay, G. P. Crawford, "Liquid crystal: Frontiers in Biomedical applications", World scientific publication Co. Pte. Ltd. (2007)